# Temporal and spectral shaping of broadband terahertz pulses in a photoexcited semiconductor

Article (Published Version)

# Temporal and spectral shaping of broadband terahertz pulses in a photoexcited semiconductor

Mostafa Shalaby' , Marco Peccianti, David G. Cooke, Christoph P. Hauri, and Roberto Morandotti'

Citation: Appl. Phys. Lett. **106**, 051110 (2015); doi: 10.1063/1.4907635
View online: http://dx.doi.org/10.1063/1.4907635
View Table of Contents: http://aip.scitation.org/toc/apl/106/5
Published by the American Institute of Physics

APPLIED PHYSICS LETTERS **106**, 051110 (2015)

# Temporal and spectral shaping of broadband terahertz pulses in a photoexcited semiconductor

Mostafa Shalaby,[1,2,a)] Marco Peccianti,[3] David G. Cooke,[4] Christoph P. Hauri,[2,5] and Roberto Morandotti[1,a)]
[1]*INRS-EMT, Varennes, Quebec J3X 1S2, Canada*
[2]*SwissFEL, Paul Scherrer Institute, 5232 Villigen PSI, Switzerland*
[3]*Department of Physics and Astronomy, University of Sussex, Pevensey Building II, 3A8, Falmer, Brighton BN1 9QH, United Kingdom*
[4]*Department of Physics, McGill University, 3600 rue University, Montréal, Québec H3A 2T8, Canada*
[5]*Ecole Polytechnique Federale de Lausanne, 1015 Lausanne, Switzerland*

(Received 25 September 2014; accepted 26 January 2015; published online 5 February 2015)

Transmission through a photoexcited semiconductor is used to temporally and spectrally shape a terahertz (THz) pulse. By adjusting the optical pump-THz probe delay, we experimentally introduce a polar asymmetry in the pulse profile as large as 92%. To shape the spectrum, we apply the same technique after strongly chirping the terahertz pulse. This leads to significant reshaping of the spectrum resulting in a 52% upshift of its median value. The pulse shaping techniques introduced here are of particular importance for temporal and spectral shape-sensitive THz nonlinear experiments. © *2015 AIP Publishing LLC*. [http://dx.doi.org/10.1063/1.4907635]

The development of high energy terahertz (THz) pulses has created the possibility for time-domain nonlinear spectroscopy with phase stable pulses in the extreme far infrared, revealing field-driven coherent dynamics of charges and spins.[1–7] In particular, a number of THz-induced nonlinear mechanisms show a strong dependence on the spectral content or the envelope function rather than on the field profile of the pulse.[2] However, in some cases, the output field shape obtained from current THz sources needs to be tailored to suit the requirements of a particular experiment. For example, in ferroelectric materials, properly shaped THz pulses can coherently guide ions over a collective microscopic path.[6] A half cycle THz pulse (a pulse with a significant asymmetry between the amplitudes of the positive and negative parts of the oscillating fields) has been predicted to induce molecular reorientation.[8] Techniques to generate intense THz pulses have developed rapidly over the past few years with field strengths peaking on the GV/m level based on both high intensity laser systems[9–12] and linear accelerators.[13] Current progress is supported by several advances in both field enhancement[14,15] and polarization manipulation.[16,17]

THz pulse shaping has been addressed in the literature by judiciously manipulating the generation process.[18–21] However, shaping the pulse during generation has been mainly addressed in photoconductive antennas and periodically poled lithium niobate. Such sources are generally unsuitable for nonlinear THz experiments due to their relatively low peak field strengths. In a recent report, Sato *et al.* demonstrated strong control on the generated THz pulse by means of shaping the pulse generation; however, this technique was strongly limited by the damage threshold in the pulse shaper yielding a maximum field of 0.3 kV/cm.[22] Pulse shaping has also been achieved through linear filtering of a freely propagating THz beam in masks and waveguides.[23,24]

In this work, we present a tunable THz pulse shaping technique operating in the time domain, capable of tailoring the temporal and spectral wave contents. Our technique operates via the excitation of free carriers in semiconductors by means of the optical pump–THz probe technique.

In an optical pump-THz probe scheme applied to a semiconductor, photo-excitation leads to an increase in the charge density and thus an attenuation and reflection of a co-propagating THz pulse. If, however, the probe-pump delay $\tau$ is carefully selected (when $\tau > 0$, the pump impinges before the probe is transmitted) and the duration of the pump pulse is less than that of the THz pulse (ignoring time-dependent scattering processes that can lead to longer saturation times in conductivity), significant shaping of the THz time profile can be obtained as we show in this paper. The reshaping of the pulse temporal profile addressed here can phenomenologically thought of as the process of clipping the pulse with the induced-carrier transition curve. It is also applicable to a wide range of spectral regimes. For example, we presented preliminary results on this slicing technique in the THz range,[25] and more recently, Mayer *et al.* used a similar technique to extend pulse shaping operation in the mid infrared range.[26]

By simply modeling the charge-induced reflection, the Gabor-limit imposes a threshold on both the observable modulation time constant and the field spectral content. We assume that no frequency products originate from the process. As a result, in a transform-limited pulse, no significant change in the temporal profile or in the spectrum should take place for a given charge induced attenuation. To shape the spectrum, we deliberately induce significant chirp in the THz pulse. As different spectral components start to temporally spread over the pulse envelope, carrier-induced modulation is shown to change the spectral distribution.

The measures presented here were performed using a time-resolved optical pump/THz probe scheme. Figure 1(a) shows a diagram of the setup where the energy of a 35 fs

a)most.shalaby@gmail.com and morandotti@emt.inrs.ca

 

pulse train (centered at a $\lambda = 800\,\text{nm}$ wavelength and featured by a repetition rate of 2.5 kHz) is split between the optical pump, the THz generation, and the THz detection supply lines. Generation and detection were performed using optical rectification and electro-optical sampling, both using ZnTe crystals, respectively. The photoexcited layer is created on the surface of a 2 mm-thick high resistivity silicon wafer. Fig. 1(b) shows the waveform and the spectrum of the THz pulse transmitted through the silicon wafer. In Fig. 1(b), $A_1$, $A_2$, and $A_3$ designate the main wave peaks amplitudes. $\tau$ is the delay between the optical pump and the THz signal, assuming that $\tau = 0$ corresponds to $A_2$ being reduced by a factor of $\sqrt{2}$. In Fig. 1(b), the sample is illuminated with a 695 $\mu$J/cm$^2$ optical pulse arriving largely after the THz pulse. As we operate in a strong carrier excitation regime, a weak THz pulse attenuation is observed, given that the carrier lifetime is comparable with the period of the pump pulse train.

The THz pulse shown here is the typical one generated from optical rectification in a ZnTe crystal. A primary objective here is to increase the asymmetry in these fields, i.e., $|A_1/A_2| \gg 1$ and $|A_1/A_3| \gg 1$. Such asymmetry is difficult to achieve during the generation process but fundamental for many THz-nonlinear experiments. For example, when an oscillating symmetric pulse is to be used to trigger magnetization switching, the effective torque on the magnetic moment depends on the orientation of the applied field.[5,27] As a result, a field-symmetric pulse produces a weak net switching effect and often leads to a non-deterministic dynamics of the magnetization.

An asymmetric THz pulse is, therefore, highly desirable for this and other applications. Asymmetry is obtained here by varying $\tau$ such that the relative values of $A_2$ and $A_3$ are gradually reduced.

Figure 1(c) shows the amplitude transition curve where the peak $A_2$ is plotted against the delay $\tau$ over a period of 9 ps. $A_2$ is attenuated by >90% when the THz pulse arrives immediately after the optical pump. Pulse asymmetry is thus expected to change as $\tau$ is varied close to the temporal overlap between the probe and the pump. The asymmetry build-up process is illustrated in Fig. 1(d) where the original and modulated pulses are presented (in normalized units) for different $\tau$ points. As the delay between the optical pulse and its THz counterpart is varied, $A_3$ starts to get attenuated first, followed by $A_2$.

To evaluate the efficiency of the shaping process, we calculate the temporal intensity modulation (shaping) depth

$$M_{i1} = \frac{(A_{i1})^2 - (A_{i1}^0)^2}{(A_{i1}^0)^2}, \quad i = 2, 3, \tag{1}$$

where $A_{21}$ and $A_{31}$ are the asymmetry factors given by $A_{21} = A_2/A_1$ and $A_{31} = A_3/A_1$, respectively. Circle superscripts denote measurements on the original unmodulated pulse. The attenuation, shown in Fig. 1(d) for few $\tau$ points, is mapped using Eq. (1) into $M_{21}$ and $M_{31}$ as presented in Fig. 2(a). Modulation depths as high as 87% and 92%, respectively, are obtained. Such high modulation translates into a strong asymmetry being introduced in the THz pulse. In a typical application, the modulation process is first examined on the given pulse. Then, the desired asymmetry is obtained by selecting the right delay. We note that the modulation process relies on varying the pump-probe delay for a certain optical fluence. At a specific delay, changing the fluence leads to different charge densities and thus both the introduced THz attenuation and pulse asymmetry vary accordingly. Figure 2(b) shows the transition curve associated to $A_2$ for different optical fluences, thus representing another degree of control over the pulse asymmetry. Finally, it is noteworthy to mention that in a typical nonlinear experiment, using a transmission configuration as we do here could lead to a THz-induced nonlinearity in the semiconductor itself which further complicates the process. For a field-driven intra-band process, there is a possibility of inter-valley scattering that increases the saturation time for the maximum conductivity, potentially to times

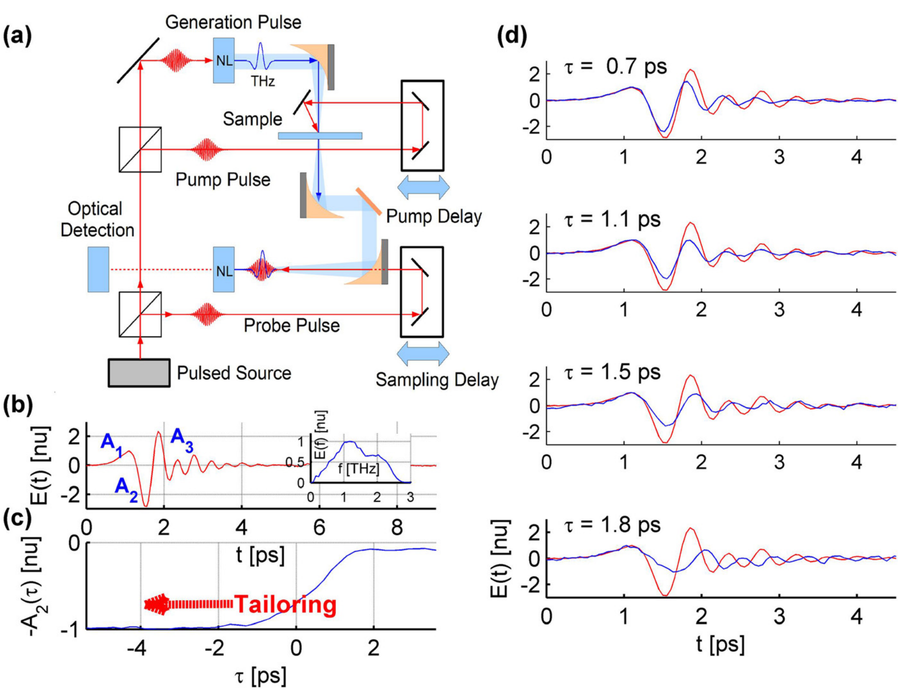


FIG. 1. (a) Schematic diagram of the optical pump/THz probe setup. (b) Time profile and spectrum of the transmitted THz pulse, arriving before the optical excitation. (c) $A_2$ amplitude transition as $\tau$ is varied. The THz amplitude transition shifted from the reference delay window shown in (c), here referred to as $\tau_0$. (d) The corresponding transmitted THz pulse (blue) for different delay times shown along with the original unmodulated pulse (red). The field amplitude is normalized to $A_1$.

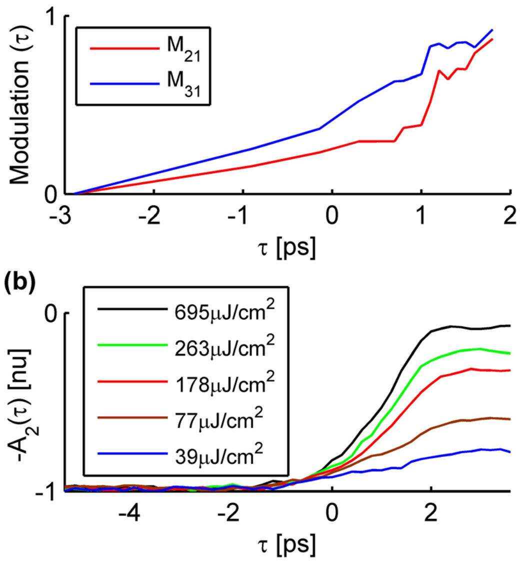


FIG. 2. (a) Intensity modulation depths $M_{21}$ and $M_{31}$ for the asymmetry factors $A_{21}$ and $A_{31}$, respectively. (b) Amplitude transition $A_2$ for different fluence levels.

longer than the pulse duration itself, detrimental to the slicing technique.[28] However, in such cases, the pulse shaping does not need to be applied in the THz focus, where the field strengths are large, but rather immediately before it in the collimated beam section where the THz field is too weak to drive nonlinearities in the semiconductor. For example, in a typical nonlinear experiment with a peak diffraction-limited field of 100 kV/cm with a 500 $\mu$m-diameter spot at the focus, the collimated beam has a spot size of 5 cm (i.e., corresponding to a peak field of 1 kV/cm), a field strength that is insufficient to induce any THz nonlinearity in the pulse shaping. Alternatively, the process can be applied in a reflection scheme. If a p-polarized THz impinges on the sample with a Brewster angle, the photo-induced reflection exhibits a complementary-shaped THz pulse.[29]

As highlighted at the beginning of our letter, a transmitted transform-limited pulse should not undergo significant spectral changes upon optical pumping. THz pulses generated using optical rectification in ZnTe are, in general, slightly chirped due to the chromatic dispersion in the crystal. This, in turn, leads to small spectral changes during the temporal shaping process. Indeed, we can achieve significant spectral shaping by chirping the THz pulse before the time slicing process. We chirped the pulse by first letting it to propagate through a copper tube of length of 278.3 mm. The inner diameter is 27.1 mm and results in an anomalous group velocity dispersion estimated to be $\beta_2 = -1.8$ ps$^2$/m at 1 THz, where higher order dispersion terms have smaller contributions. Different frequency components are therefore spread over different delays and the time slicing process can be used to filter some of them and thus shift the center of the spectrum. As the pulse is negatively chirped, high frequencies tend to survive the clipping, whereas as $\tau$ decreases, the output spectrum is progressively enriched with lower frequency contributions. Figs. 3(b) and 3(c) show the shaped time profiles and the corresponding spectra, respectively. Four sections are presented in Figs. 3(d) and 3(e). Here, the time clipping is accompanied by a significant upshift of the frequency spectral components. The change in the spectrum is clearly appreciated in Fig. 3(f) where both the spectrum center ($f_2$) and the FWHM "edge" frequencies ($f_1$ and $f_3$) are shown. All the spectra presented in Fig. 3 are in normalized units. Note that this process is accompanied by (i) a narrowing of the FWHM bandwidth and (ii) the translation of the spectrum center up in frequency. Finally, the spectral modulation parameter $M_f = 1 - (f_1)^2/(f_1^{\circ})^2$ is presented in Fig. 3(g), where a modulation as high as 52% was obtained. It should be noted that for a p-polarized THz impinging on the sample with a Brewster angle, the spectrum median is downshifted. Alternatively, low-pass filtering can be achieved by positively chirping the input pulse[30] or collecting the reflected pulse.

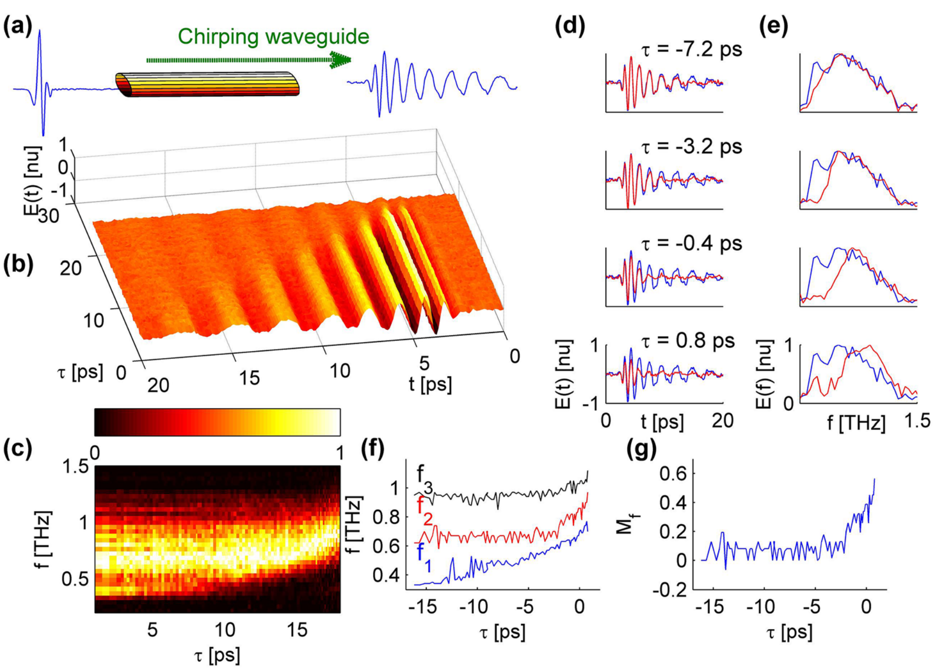


FIG. 3. (a) Negative chirping of the THz pulses under investigation. (b) Time profile and (c) spectrum of the transmitted THz pulse as the pump-probe delay is varied. Note that an arbitrary zero delay point is chosen. (d) Time profiles and (e) spectra of the modulated and unmodulated pulses at chosen delay times. (f) Trace lines of the FWHM frequency "edges" ($f_1$ and $f_3$) and spectrum median ($f_2$). (g) Spectral modulation parameter $M_f$.

In conclusion, we have shown that optical pump-THz probe generation of carriers in semiconductors can be used to temporally and spectrally shape a THz pulse. Controlling the delay between the two pulses leads to different parts of the THz pulses experiencing different attenuations and thus temporal shaping of the pulse. If the process is preceded by chirping the THz pulses, the same temporal shaping results in significant shaping of the spectrum as well. We believe that our results will help to overcome some pulse shape limitations in nonlinear THz experiments.

This work was supported in Canada by MERST, FQRNT, and NSERC. M.S. acknowledges a FQRNT MELS scholarship. M.P. acknowledges the support from the FP7 Marie Curie Actions of the European Commission, via the Career-Integration Grant (Contract No. 630833). M.S. wishes to thank Professor Tsuneyuki Ozaki and Professor Francois Légaré (INRS-EMT) for helpful discussions on THz pulse shaping.

[1]K. Tanaka, H. Hirori, and M. Nagai, IEEE Trans. Terahertz Sci. Technol. **1**, 301 (2011).
[2]M. Shalaby and C. P. Hauri, "Air nonlinear dynamics initiated by ultra-intense lambda cubic THz pulses," arXiv:1410.0219.
[3]M. Liu, H. Y. Hwang, H. Tao, A. C. Strikwerda, C. Fan, G. R. Keiser, A. J. Sternbach, K. G. West, S. Kittiwatanakul, J. Lu *et al.*, Nature **487**, 345 (2012).
[4]T. Kampfrath, K. Tanaka, and K. A. Nelson, Nat. Photonics **7**, 680 (2013).
[5]C. Vicario, C. Ruchert, F. Ardana-Lamas, P. M. Derlet, B. Tudu, J. Luning, and C. P. Hauri, Nat. Photonics **7**, 720 (2013).
[6]T. Qi, Y.-H. Shin, K.-L. Yeh, K. A. Nelson, and A. M. Rappe, Phys. Rev. Lett. **102**, 247603 (2009).
[7]W. Ronny, E. A. Nanni, K. Ravi, K.-H. Hong, L. J. Wong, P. D. Keathley, A. Fallahi, L. Zapata, and F. X. Kartner, "A terahertz-driven electron gun," arXiv:1409.8668.
[8]M. Machholm and N. Henriksen, Phys. Rev. Lett. **87**, 193001 (2001).
[9]C. P. Hauri, C. Ruchert, C. Vicario, and F. Ardana, Appl. Phys. Lett. **99**, 161116 (2011).
[10]M. Clerici, M. Peccianti, B. E. Schmidt, L. Caspani, M. Shalaby, M. Giguere, A. Lotti, A. Couairon, F. Legare, T. Ozaki *et al.*, Phys. Rev. Lett. **110**, 253901 (2013).
[11]A. Gopal, S. Herzer, A. Schmidt, P. Singh, A. Reinhard, W. Zeigler, D. Brommel, A. Karmakar, P. Gibbon, U. Dilner *et al.*, Phys. Rev. Lett. **111**, 074802 (2013).
[12]M. Shalaby and C. P. Hauri, Nat. Commun. **6**, 5976 (2015).
[13]D. Daranciang, J. Goodfellow, M. Fuchs, H. Wen, S. Ghimire, D. Reis, H. Loos, A. S. Fisher, and A. M. Lindenberg, Appl. Phys. Lett. **99**, 141117 (2011).
[14]M. Seo, H. R. Park, S. M. Koo, D. J. Park, J. H. Kang, O. K. Suwal, S. S. Choi, P. C. M. Planken, G. S. Park, N. K. Park *et al.*, Nat. Photonics **3**, 152 (2009).
[15]M. Shalaby, J. Fabianska, M. Peccianti, Y. Ozturk, F. Vidal, H. Sigg, R. Morandotti, and T. Feurer, Appl. Phys. Lett. **104**, 171115 (2014).
[16]A. Shuvaev, V. Dziom, A. Pimenov, M. Schiebl, A. A. Mukhin, A. C. Koramerk, T. Finger, M. Braden, and A. Pimenov, Phys. Rev. Lett. **111**, 227201 (2013).
[17]M. Shalaby, M. Peccianti, Y. Ozturk, and R. Morandotti, Nat. Commun. **4**, 1558 (2013).
[18]C. Ludwig and J. Kuhl, Appl. Phys. Lett. **69**, 1194 (1996).
[19]S. Vidal, J. Degert, J. Oberle, and E. Freysz, J. Opt. Soc. Am. B **27**, 1044 (2010).
[20]W. C. Hurlbut, B. J. Norton, N. Amer, and Y.-S. Lee, J. Opt. Soc. Am. B **23**, 90 (2006).
[21]A. Stepanov, J. Hebling, and J. Kuhl, Opt. Express **12**, 4650 (2004).
[22]M. Sato, T. Higuchi, N. Kanda, K. Konishi, K. Yoshioka, T. Suzuki, K. Misawa, and M. Kuwata-Gonokami, Nat. Photonics **7**, 724 (2013).
[23]E. S. Lee, S. G. Lee, C. S. Kee, and T. I. Jeon, Opt. Express **19**, 14852 (2011).
[24]J. Bromage, S. Radic, G. P. Agrawal, C. R. Stroud, P. M. Fauchet, and R. Sobolewski, Opt. Lett. **22**, 627 (1997).
[25]M. Shalaby, M. Peccianti, L. Razzari, G. Sharma, T. Ozaki, and R. Morandotti, *Ultrafast THz Pulse Shaping: Generation of Half-Cycle Pulse From Multi-Cycle THz Pulse* (Optical Sensors: Terahertz Waveguides, Applications, and Device Technology, Toronto, Canada, 2011).
[26]B. Mayer, C. Schmidt, J. Buhler, D. V. Seletskiy, D. Brida, A. Pashkin, and A. Leitenstorfer, New J. Phys. **16**, 063033 (2014).
[27]M. Shalaby, F. Vidal, M. Peccianti, R. Morandotti, F. Enderli, T. Feurer, and B. D. Patterson, Phys. Rev. B **88**, 140301(R) (2013).
[28]R. Ulbricht, E. Hendry, J. Shan, T. F. Heinz, and M. Bonn, Rev. Mod. Phys. **83**, 543 (2011).
[29]F. A. Hegmann and M. S. Sherwin, Proc. SPIE **2842**, 90 (1996).
[30]R. Mendis and D. Grischkowsky, J. Appl. Phys. **88**, 4449 (2000).